

## CFD-MODELLING FOR THE COMBUSTION OF SOLID BALED BIOMASS

Martin MILTNER, Aleksander MAKARUK, Michael HARASEK and Anton FRIEDL

Vienna University of Technology, Institute of Chemical Engineering, Getreidemarkt 9/1662, 1060 Vienna, Austria

### ABSTRACT

The importance of biomass in combustion processes for the combined production of electrical power and district heat is still rising. In the presented work, Computational Fluid Dynamics is used for the development and optimisation of an innovative combustion chamber for a solid stem-shaped biofuel in the form of compressed biomass bales. The main focus of this investigation is the maximisation of the thermal output of the combustor by an optimisation of the bale burnout and the minimisation of gaseous emissions such as VOCs, carbon monoxide and nitrogen oxide. For this purpose the functionality of a commercial CFD-solver has been extended using user-defined functions for the characterisation of the solid phase and the solid-gas-interactions. These sub-routines comprise the description of the solid biomass fuel as a porous bed, the biomass drying, the degradation during devolatilisation and char burnout, as well as the generation of gaseous species and the release/consumption of energy during these three steps. Moreover a simplified model for the prediction of nitrogen oxide emissions emanating from the fuel-bound nitrogen has been implemented.

The results of the present work show that the application of CFD enables a significant reduction of the development costs and the time-to-market of innovative chemical engineering concepts such as solid biomass combustion.

### NOMENCLATURE

$A$	Arrhenius pre-exponential factor
$A_{spec}$	Specific surface of the char particles
$D$	Molecular diffusion coefficient
$d_p$	Char particle diameter
$E$	Arrhenius activation energy
$k$	Kinetic constant
$MG$	Molecular weight
$p_{O_2}$	Oxygen partial pressure
$r$	Chemical reaction rate
$T$	Temperature
$V_{Cell}$	Volume of a discrete control cell
$v$	Gas velocity
$x$	Species mass content
$\varepsilon$	Char bed porosity
$\Phi$	Char combustion stoichiometric ratio
$\rho$	Density
$\mu$	Dynamic viscosity

### INTRODUCTION

During the last decades the utilisation of biomass for combustion processes gained more and more importance in the field of combined production of electrical power and district heat. This is a result of an increasing CO<sub>2</sub>-awareness and high prices for fossil fuels. The development of appropriate combustion concepts for biomass fuels is rather challenging and often time- and

cost-intensive because of the heterogeneous composition and disadvantageous ash melting behaviour of the considered biomass. Therefore, the application of modern simulation tools, like Computational Fluid Dynamics (CFD), can be of vital importance for the project.

In the present work, CFD is used for the development and optimisation of an innovative combustion chamber for a solid biomass in the form of compressed bales of whole crop maize. The modelling approaches that have to be applied to obtain qualitatively and quantitatively meaningful results are outlined. The main objective of this investigation is the minimisation of the gaseous emissions such as Volatile Organic Components (VOCs), carbon monoxide and nitrogen oxide. Furthermore, the thermal output of the apparatus shall be maximised by an optimisation of the bale burnout.

The simulations are accompanied by extensive combustion experiments carried out at a medium scale pilot plant with 2MW thermal output. The combustion chamber of this plant currently makes use of an innovative concept of staged biomass combustion. The results of these experiments enabled the comparison and calibration of the calculation models and their parameters.

### MODEL DESCRIPTION

In the following section a short introduction to the applied models is given. The main focus lies in the description of the heterogeneous reaction steps during solid biomass combustion. A drawing of the principal modelling approach regarding this issue is given in Figure 1 which was adapted from Zhou et al. (2005).

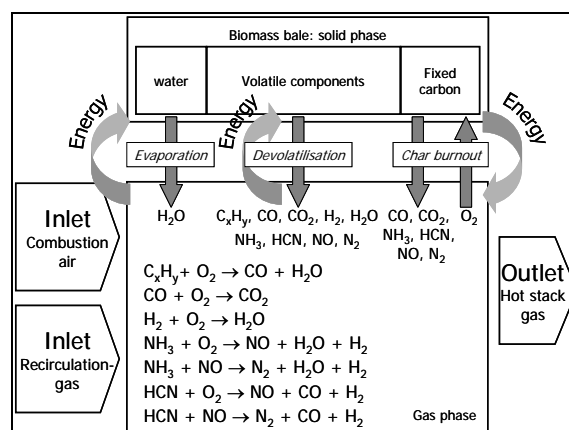


**Figure 1:** Overview of the chemical reaction scheme concerning heterogeneous biomass combustion (see Table 1 for stoichiometric parameters)

Some of the applied standard modelling approaches are only shortly introduced here; a more detailed description has recently been given by Miltner et al. (2006).

### General modelling approach

The CFD calculations presented in the current work have been accomplished using the commercial RANS-CFD-Solver FLUENT 6.2 with the geometrical pre-processor GAMBIT 2.2. Turbulence has been modelled using the SST-k- $\omega$ -turbulence model by Menter (1994) because of its good performance in preliminary investigations of turbulent swirling free-jets. The solid regions of the biomass bale as well as the char bed are treated as a porous zone with defined flow resistance. For the description of the radiative heat transfer the Discrete Ordinates model (DO) combined with the WSGGM model for the gas absorption characteristics has been chosen. All heterogeneous reaction steps have been implemented and the governing equations have been solved iteratively using an external Newton-solver. The results have been transferred to FLUENT using user-defined subroutines.

### Homogeneous gas reactions

For the description of the composition of the gaseous regions inside the combustor the so-called species-transport-approach has been used. For this purpose ten 'command' species have been defined (given in Figure 1). These species participate in seven homogeneous gas reactions that are assumed to describe the combustion process sufficiently. The stoichiometry of these reactions is given in Table 1. The reaction rate expressions for the mentioned reactions are given in Table 2.

#	Reaction
H1	$H_2 + 0,5 O_2 \rightarrow H_2O$
H2	$CO + 0,5 O_2 \rightarrow CO_2$
H3	$C_x H_y + \left(\frac{x}{2} + \frac{y}{4}\right) O_2 \rightarrow x CO + \frac{y}{2} H_2O$
H4	$NH_3 + O_2 \rightarrow NO + H_2O + 0,5 H_2$
H5	$NH_3 + NO \rightarrow N_2 + H_2O + 0,5 H_2$
H6	$HCN + O_2 \rightarrow NO + CO + 0,5 H_2$
H7	$HCN + NO \rightarrow N_2 + CO + 0,5 H_2$

**Table 1:** Stoichiometry for the homogeneous gas-phase reactions.

#	Rate expression	Parameters
H1	$k_{H2} [H_2] \times [O_2]$	$k_{H2} = 9,87 \times 10^8 \exp\left(-\frac{3728,4}{T}\right)$
H2	$k_{CO} [CO] \times [O_2]^{0,25} \times [H_2O]^{0,5}$	$k_{CO} = 2,239 \times 10^{12} \exp\left(-\frac{20446,3}{T}\right)$
H3	$k_{CxHy} [C_x H_y]^{0,2769} \times [O_2]^{1,3632}$	$k_{CxHy} = 1,0729 \times 10^{10} \exp\left(-\frac{15311,8}{T}\right)$
H4	$k_{NH3} [NH_3] \times [O_2]^{0,5} \times [H_2]^{0,5}$	$k_{NH3} = 1,21 \times 10^5 \times T^2 \exp\left(-\frac{8000}{T}\right)$
H5	$k_{NH3} [NH_3] \times [NO]$	$k_{NH3} = 8,73 \times 10^{14} \times T^{-1} \exp\left(-\frac{8000}{T}\right)$
H6	$k_{HCN} [HCN] \times [O_2]$	$k_{HCN} = 1,0 \times 10^{10} \exp\left(-\frac{33712}{T}\right)$
H7	$k_{HCN} [HCN] \times [NO]$	$k_{HCN} = 3,0 \times 10^{12} \exp\left(-\frac{30188}{T}\right)$

**Table 2:** Rate expression for homogeneous gas-phase reactions.

We followed the suggestions of Zhou et al. (2005) to keep the reaction scheme as simple as possible to enhance the numerical stability and the convergence behaviour. The water shift reaction applied for example in Fletcher et al.

(2000) is assumed to be of minor importance in this application due to the higher equivalence ratio of a combustor compared to a gasifier. However, more comprehensive mechanisms with a higher number of chemical reactions are currently under investigation. The kinetic parameters for the mentioned homogeneous gas-phase reactions have been taken from Brink et al. (2001), Hill et al. (2000) and from the FLUENT Users Guide (2005).

The chemistry-turbulence coupling for the homogeneous gas-phase reactions has been accomplished using the Eddy Dissipation Concept by Magnussen and Hjertager (1976).

### Moisture evaporation

The evaporation of the biomass moisture has been analysed by preliminary TGA measurements. Based on this analysis the conversion from liquid to gaseous water is assumed to be a first-order reaction with a modified Arrhenius approach for the description of the influence of the solid biomass temperature:

$$\frac{\partial [H_2O]_{liquid}}{\partial t} = -k_{H2O} \times [T - 475]^7 \times [H_2O]_{liquid} \quad (1)$$

$$k_{H2O} = 2,822 \times 10^{-4} \times \exp\left(-\frac{10584}{T_{solid}}\right) \quad (2)$$

### Devolatilisation

Compared to coal, biomass contains a high amount of volatile components (up to 75 wt%), that are gasified during the devolatilisation phase. The composition of the gaseous volatiles has been taken from Adanez et al. (2003) and was slightly adapted to fit the ultimate and proximate analysis of the biomass fuel. The species used in this approach are CO, CO<sub>2</sub>, H<sub>2</sub>, H<sub>2</sub>O, a pseudo-species C<sub>x</sub>H<sub>y</sub> containing higher hydrocarbons and some precursor species for fuel-bound NO<sub>x</sub> emissions. The thermal degradation rate of the solid biomass fuel has also been analysed by preliminary TGA measurements. A lumped parameter model with three pseudo-components (Cellulose, Hemicellulose, and Lignin) has been applied. The conversion rates of these components to gaseous volatiles and solid residual char have been modelled as first order reactions in terms of the residual mass of the specified component together with an Arrhenius approach for the solid temperature influence:

$$\frac{\partial m_i}{\partial t} = k_i \times (m_i^0 - m_i) \quad \text{with: } m_i^0 = m_i^0 \times x_i^0 \quad (3)$$

$$k_i = A_i \times \exp\left(-\frac{E_i}{R \times T_{solid}}\right) \quad (4)$$

The parameters for this lumped devolatilisation model have been adapted to fit the TGA measurements and are given in Table 3.

	$x_i^0$ [wt% (daf)]	$x_i^\infty$ [wt%]	$A_i$	$E_i$ [J/mol]
Cellulose	40.83	2.82	$9,00 \times 10^{11}$	$1,285 \times 10^5$
Hemicellulose	34.93	29.93	$3,74 \times 10^5$	$7,547 \times 10^4$
Lignin	24.24	38.00	$1,6 \times 10^{-3}$	$1,500 \times 10^4$

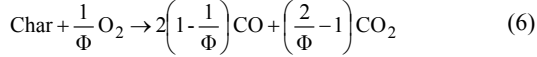
**Table 3:** Model parameters for the lumped devolatilisation model.

Together with the progressive formation of volatile gases the generation of residual char arising from the individual pseudo-components can be described as follows:

$$\left(\frac{\partial m_{Char}}{\partial t}\right)_{formation} = -\sum_i \left(\frac{m_i^\infty}{m_i^0 - m_i^\infty}\right) \times \frac{\partial m_i}{\partial t} \quad (5)$$

### Char burnout

The char forms as volatiles escape from the biomass particles and is burned during the char combustion phase with consumption of oxygen. With the assumption that char only contains carbon, the char oxidation reaction is:



In this reaction the stoichiometric ratio for the char combustion is defined as follows:

$$\Phi = \frac{1 + [CO_2]/[CO]}{0.5 + [CO_2]/[CO]} \quad (7)$$

The ratio of CO to CO<sub>2</sub> during char combustion is a function of the char particle temperature and has been estimated by Zhou et al. (2005):

$$\frac{[CO]}{[CO_2]} = 12 \times \exp\left(-\frac{3300}{T_{Char}}\right) \quad (8)$$

The char combustion rate is controlled by gas film diffusion and by chemical reaction. Following the works of van der Lans et al. (2000), Zolin et al. (2002), and Zhou et al. (2005), the rate of biomass char combustion under chemical reaction control can be derived from TGA measurements. Fitted to a first order reaction in terms of oxygen partial pressure and residual char mass the equation for this reaction regime reads as follows:

$$\left(\frac{\partial m_{Char}}{\partial t}\right)_{kinetic} = k_{kinetic} \times p_{O_2} \times m_{Char} \quad (9)$$

$$k_{kinetic} = 0.648593 \times \exp\left(-\frac{15907}{T_{Char}}\right) \quad (10)$$

To account for the film diffusion of the oxygen species a correlation between gas flow and mass transfer in terms of the Colburn factor as introduced by Dwivedi et al. (1977) is used:

$$\varepsilon \times J = \frac{0.765}{Re_d^{0.82}} + \frac{0.365}{Re_d^{0.386}} \quad (11)$$

Where the Colburn factor is defined as:

$$J = \frac{Sh_d}{Sc^{1/3} \times Re_d} \quad (12)$$

In this equation the Sherwood number, Schmidt number, and Reynolds number are defined as follows:

$$Sh_d = \frac{k_{Film} \times d_p}{D} \quad (13)$$

$$Sc = \frac{\mu_{Gas}}{\rho_{Gas} \times D} \quad (14)$$

$$Re_d = \frac{v_{Gas} \times d_p \times \rho_{Gas}}{\mu_{Gas}} \quad (15)$$

Using the definition of the stoichiometric ratio of the char combustion the char burnout reaction rate under film diffusion control can be developed:

$$\left(\frac{\partial m_{Char}}{\partial t}\right)_{Film} = k_{Film} \times \frac{p_{O_2}^{Gas} - p_{O_2}^{Surf}}{R \times T_{Char}} \times \Phi \times MG_{Char} \times A_{spec} \times V_{Cell} \quad (16)$$

$$k_{Film} = \frac{D^{2/3} \times v_{Gas} \times \rho^{2/3}}{\mu_{Gas}^{2/3} \times \varepsilon} \times \left(\frac{0.765}{Re_d^{0.82}} + \frac{0.365}{Re_d^{0.386}}\right) \quad (17)$$

In the latter equation the molecular diffusion coefficient of oxygen in air has been calculated by the equations of Wilke & Lee given in Reid et al. (1987). The porosity and several thermal properties of the char bed have been estimated using experimental results from Fjellerup and Henriksen (2003).

Kinetic char oxidation rate and film diffusion reaction rate have been combined to form the overall char consumption rate introducing an effective reaction rate constant:

$$\frac{\partial m_{Char}}{\partial t} = k_{eff} \times p_{O_2}^{Gas} \times m_{Char} \quad (18)$$

$$k_{eff} = \frac{1}{\frac{1}{k_{kinetic}} + \frac{1}{k_{Film} \times MG_{Char} \times \Phi \times A_{spec} \times V_{Cell}}} \quad (19)$$

Together with the energy balance, the overall mass balance of char containing a sink for oxygen and a source of CO and CO<sub>2</sub> had to be solved for each discrete volume cell of the char burnout region.

### Nitrogen oxide emissions

Due to the fact that the gas temperature inside the combustion system has to be kept below 850°C to avoid slagging and fouling, thermal mechanisms of nitrogen oxide formation can be neglected according to the works of Glassman (1996). In order to estimate the nitrogen oxide emissions emanating from the fuel-bound nitrogen, a simplified model has been developed. Additionally to the above mentioned reaction products of the heterogeneous reaction steps of devolatilisation and char combustion so-called NO<sub>x</sub> precursor species are assumed to be emitted from the solid. These four nitrogen-containing species are NH<sub>3</sub>, HCN, NO and N<sub>2</sub>. The formation characteristics of these substances have been analysed by Winter et al. (1999) and have been adapted to the current application. According to the progress of the devolatilisation and the char combustion steps these species are emitted to the gas-phase and run through the previously defined homogeneous chemical reactions.

## RESULTS

In the following section, a short overview of the simulation results is given. Firstly, the homogeneous gas reaction mechanism will be analysed by doing a parameter study. In a second step, the solid biomass combustion model will be examined using a simplified combustor geometry. These simulation works together with an extended model parameter optimisation is still ongoing.

### Analysis of the homogeneous gas reaction mechanism

To verify the applicability and abilities of the newly introduced homogeneous gas reaction mechanism in combination with the simplified NO<sub>x</sub> emission model, an

extensive parameter study concerning the oxygen content has been conducted. For this reason, the mechanism has been applied to the CFD-model of an idealised non-isothermal Plug Flow Reactor (PFR). The inlet conditions of this testcase have been chosen to fit the conditions of the postcombustion zone in the real combustor approximately.

The result of one CFD calculation is given in Figure 2. For this calculation, an initial oxygen content of 6.5 mol% (corresponding to an overall equivalence ratio of 1.016) has been chosen. The diagram shows the residual molar fractions (actual molar fraction related to initial molar fraction) of the leading species as well as the gas temperature versus the residence time in the PFR. It is observable that the main part of the reaction occurs within the first half second. The temperature rises from 950 to 1700K which has a strong influence on the chemical reaction rates. In the real combustor this effect would of course be immediately compensated by the addition of recirculation gas to keep the temperature below 1100K. The oxidation of the combustible carbon-species moves on, whereas the quantity of nitrogen oxide aspires to a constant value.

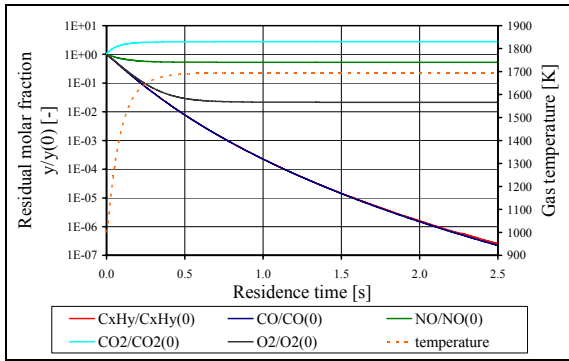


**Figure 2:** Residual molar fractions of the leading species and gas temperature along the reaction pathway in an idealised non-isothermal PFR (Oxygen equivalence ratio 1.016, initial gas temperature 950K).

A summary of the results of the parameter variation is given in Figure 3. This diagram shows the residual molar fractions of  $C_xH_y$ , CO and NO after one second of reaction in the PFR at different initial oxygen contents (corresponding to a certain overall equivalence ratio). The ideal behaviour of the plug flow reactor is reflected in the fact that the residual amount of combustible carbon-species is almost zero at equivalence ratios higher than 1 (complete combustion takes place). If not enough oxygen is provided, the residual amount of combustibles in the off-gas rises. The oxidation of  $C_xH_y$  seems to be more sensitive to a lack of oxygen than the carbon monoxide oxidation reaction. The pseudo-species  $C_xH_y$  represent a part of the VOCs in this model. The emissions of these substances are usually strongly limited by legislation especially for low-temperature biomass combustion facilities. With a decreasing amount of excess oxygen the emission of nitrogen oxide can be reduced. Keeping this behaviour in mind, an optimised equivalence ratio can be expected, in order to minimise both the emissions of unburnt carbon-species and nitrogen oxide.

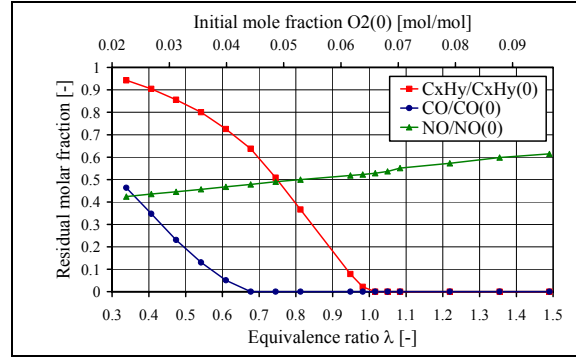


**Figure 3:** Residual molar fractions of  $C_xH_y$ , CO and NO after 1 second of reaction in an idealised non-isothermal PFR at different initial oxygen contents.

A further investigation concerning the reaction rate constants of the N-species will be necessary due to the fact that the current model seems to slightly underestimate the influence of the oxygen content on the amount of nitrogen oxide as it has been observed during combustion experiments at the pilot plant.

#### Analysis of the solid biomass combustion model

For the development and parameterisation of the solid biomass combustion model, the original geometry of the combustion chamber has been simplified. Nevertheless, the fluid dynamic mean residence time and the main features of the original design have been kept constant. A drawing of this geometry is given in Figure 4.

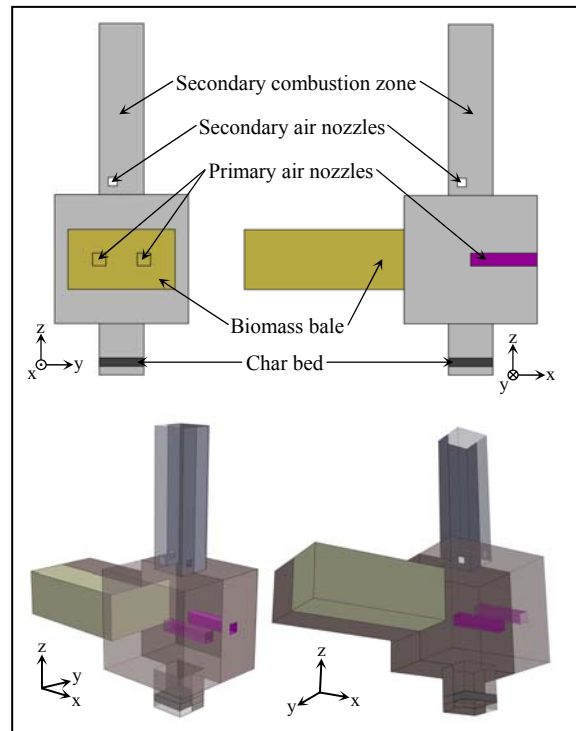


**Figure 4:** Drawing of the simplified combustion chamber for model development.

Two different combustion chamber operation modes have been analysed, distinguishing each other by the amount of air supply to the primary air nozzles. Details about the boundary conditions of the considered two cases are given in Table 4.

	CASE 1	CASE 2
Thermal input [kW]	2180	2180
Overall equivalence ratio [-]	1.743	1.743
Mass flow combustion air [kg/s]	1.32	1.32
Mass flow recirculation gas [kg/s]	1.49	1.49
Primary air fraction [-]	0.55	0.50
Secondary air fraction [-]	0.3	0.35
Afterburning grate air fraction [-]	0.15	0.15
Oxygen mass flow primary [kg/s]	0.199	0.184
Oxygen mass flow secondary [kg/s]	0.179	0.194

**Table 4:** Boundary conditions of the two analysed combustion chamber operation modes.

Attentive investigation of the CFD calculations reveals that the  $\text{NO}_x$ -emission of CASE1 amounts to  $166\text{mgNO}_2/\text{m}^3\text{STP}$ , while CASE2 shows only  $159\text{mgNO}_2/\text{m}^3\text{STP}$  (-4%). However, the amount of carbon monoxide emission of CASE2 is  $900\text{mg}/\text{m}^3\text{STP}$ , while CASE1 shows only  $800\text{mg}/\text{m}^3\text{STP}$  (+11% for CASE2). Moreover, the degree of char burnout is worse for CASE2, showing 1.05wt% of char, while the char burnout is complete for CASE1.

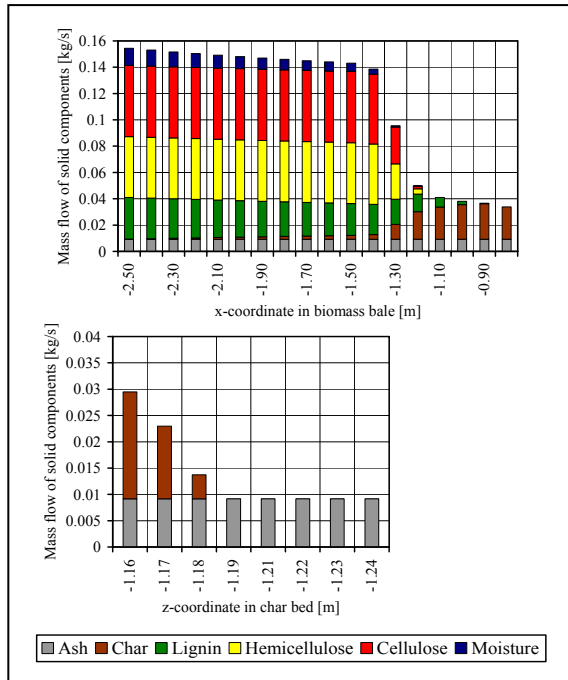


**Figure 5:** Mass flow of the solid components along the biomass bale and the char bed.

Figure 5 shows the mass flow of solid components in the solid phase for CASE1. The volatilisation of the biogenic pseudo-species Cellulose, Hemicellulose and Lignin taking place with different reaction rates is clearly distinguishable. The amount of char in the solid phase increases with progressing devolatilisation. The char combustion initiates almost at the end of the devolatilisation step. It can be seen, that the char combustion is finished rather early in the char bed (at a z-coordinate of -1.19). It is supposed, that this reaction rate is slightly overestimated and an optimisation of the char combustion parameters is still necessary.

The contents of volatile species and char in the bale and in the char bed for CASE1 are depicted in Figure 6. It has to

be mentioned, that the moisture is not included in the sum of volatile components in this analysis. It can be observed, that the devolatilisation process spans a quite large extent and that the duration of this process is rather long. The char burnout reaction, which is starting already inside the bale volume, needs a minimum particle temperature of about 1000K together with a sufficient amount of oxygen for initiation.

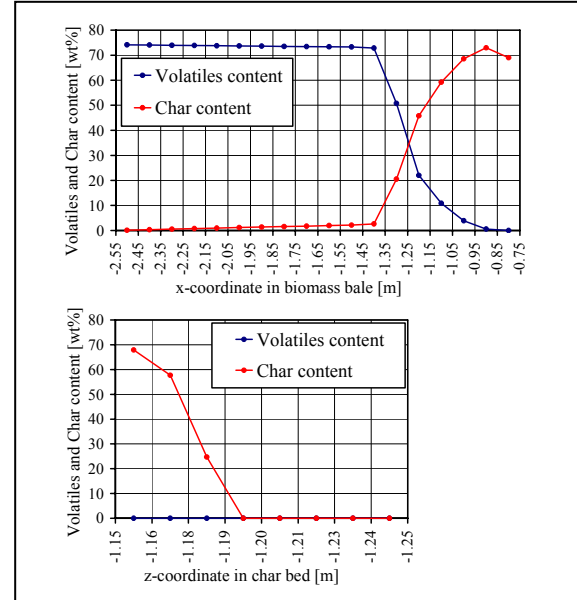


**Figure 6:** Content of volatiles and char along the biomass bale and the char bed.

Finally, a glance inside the computational domain of the combustor shall be made to give an overview of the flow field characteristics of the innovative combustion concept.

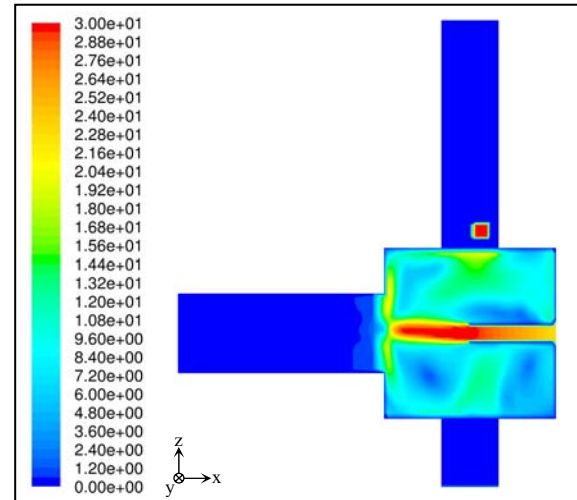


**Figure 7:** Contours of gas velocity magnitude on a cut plane through a primary air nozzle (0 – 30m/s).

Figure 7 shows a contour plot of the gas velocity magnitude on a vertical cut plane through the combustor. The impact of the primary air nozzles on the bale surface and the induced turbulence is clearly observable.

Figure 8 shows a contour plot of the gas temperature on the same cut plane through the combustor. The cold

impinging primary air jets are clearly visible as well as a hot stream emanating from the combustive char bed in the afterburner zone. The temperature profile inside the bale and in the vicinity of the bale surface provides valuable information about the burnout characteristics for a further optimisation and performance enhancements.

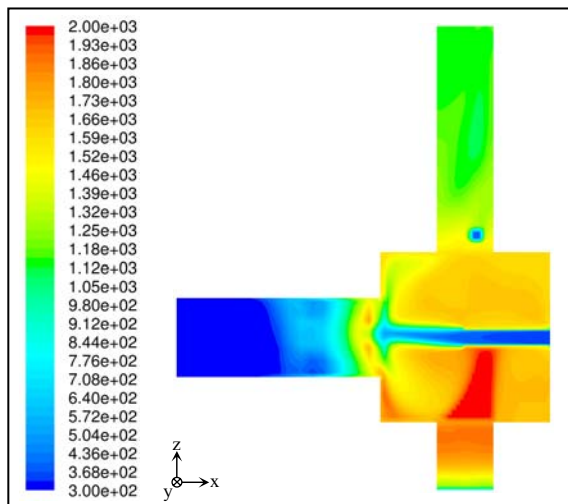


**Figure 8:** Contours of gas temperature on a cut plane through a primary air nozzle (300 – 2000K).

## CONCLUSIONS

The results of the present work give an overview of the capabilities of CFD in the field of solid biomass combustion. If this tool is applied in an early stage of the project, time- and cost-intensive experimental investigations could be reduced. Furthermore, attentive analysis of the results provides a deeper insight in the physical and thermal behaviour of the considered apparatuses and processes.

In order to generate meaningful results, one has to apply concise and sharpened modelling approaches with verified modelling parameters. This work gives a short overview of the models that have to be considered and how an implementation into available commercial software could be done.

The generated results can be used to optimise the combustion chamber design and the operational parameters. The flue gas recirculation rate and the overall equivalence ratio can be varied in order to reduce gaseous emissions of CO and NO<sub>x</sub>. Several constructive details of the combustion chamber can be analysed for a further reduction of these emissions. Examination of the predicted biomass bale burnout can be a great help for the maximisation of the thermal output of the combustor. The calculated combustion chamber wall temperatures can be used for choosing the proper steel grade for the shell as well as for the identification of slagging and temperature corrosion sources. Attentive analysis of the calculated flow field inside the combustion chamber enables the determination of flow dead zones (danger of ash deposition) and vortices (unwanted back mixing and disadvantageous residence time distribution). Thus, the combustion chamber itself as well as the whole combustion cycle can be tailored to the essential dimensions without an expensive experimental evaluation.

However, some of the modelling approaches and model parameters still require further investigation. The reaction rate of the char burnout reaction will be further analysed to improve the model predictions. The composition of the volatile gases and their formation during devolatilisation will be investigated. The target is to find a model with an operation-dependent composition of the volatile gases and the nitrogen oxide precursor substances. The presented model comprises constant generation characteristics, which is a significant simplification. Additionally, refined Arrhenius parameters for the N-species reactions have to be found. The parameter set taken from literature seems to underestimate the influence of the oxygen content on the generation of nitrogen oxide. Finally, the applied models will undergo comprehensive sensitivity analyses to check for their physical relevance.

## REFERENCES

- ADANEZ, J. et al., (2003), "Combustion of wood chips in a CFBC: modelling and validation", *Ind. Eng. Chem. Res.*, **42**, 987-999.
- BRINK, A., KILPINEN, P., HUPA, M., (2001), "A simplified kinetic rate expression for describing the oxidation of volatile fuel-N in biomass combustion", *Energy & Fuels*, **15**, 1094-1099.
- DWIVEDI, P.N. and UPADHYAY, S.N., (1977), "Particle-Fluid mass transfer in fixed and fluidized beds", *Ind. Eng. Chem. Process Des. Dev.*, **16**, 157-165.
- FJELLERUP, J. and HENRIKSEN, U., (2003), "Heat transfer in a fixed bed of straw char", *Energy & Fuels*, **17**, 1251-1258.
- FLETCHER, D.F. et al., (2000), "A CFD based combustion model of an entrained flow biomass gasifier", *Appl. Math. Modelling*, **24**, 165-182.
- FLUENT 6 Users Guide, (2005), FLUENT Inc.
- GLASSMAN, I., (1996), "Combustion", 3<sup>rd</sup> edition, Academic Press San Diego, 373-383.
- HILL, S.C., SMOOT, L.D., (2000), "Modelling of nitrogen oxides formation and destruction in combustion systems", *Prog. Energ. Combust. Sci.*, **26**, 417-458.
- MAGNUSSEN, B.F. and HJERTAGER, B.H., (1976), "On mathematical models of turbulent combustion with special emphasis on soot formation and combustion", *16<sup>th</sup> Symposium on Combustion*, The Combustion Institute.
- MENTER, F.R., (1994), "Two-equation Eddy-viscosity turbulence models for engineering applications", *AIAA J.*, **32**, 1598-1605.
- MILTNER, M. et al., (2006), "Process simulation and CFD calculations for the development of an innovative baled biomass-fired combustion chamber", *Appl. Therm. Eng.*, in press.
- REID, R.C., PRAUSNITZ, J.M. and POLING, B.E., (1987), "The properties of gases & liquids", 4<sup>th</sup> edition, McGraw-Hill New York, 586-631.
- VAN DER LANS, R.P. et al., (2000), "Modelling and experiments of straw combustion in a grate furnace", *Biomass and Bioenergy*, **19**, 199-208.
- WINTER, F., WARTHA, C., HOFBAUER, H., (1999), "NO and N<sub>2</sub>O formation during the combustion of wood, straw, malt waste and peat", *Bioresour. Technol.*, **70**, 39-49.
- ZHOU, H. et al., (2005), "Numerical modelling of straw combustion in a fixed bed", *Fuel*, **84**, 389-403.
- ZOLIN, A. et al., (2002), "Experimental study of char thermal deactivation", *Fuel*, **81**, 1065-1075.